

TECHNICAL ADVANCE

Quantification of plant surface metabolites by matrix-assisted laser desorption–ionization mass spectrometry imaging: glucosinolates on *Arabidopsis thaliana* leaves

Rohit Shroff^{1,†}, Katharina Schramm^{2,†,‡}, Verena Jeschke², Peter Nemes³, Akos Vertes³, Jonathan Gershenzon^{2,*} and Aleš Svatoš¹

¹Research Group on Mass Spectrometry/Proteomics, Max Planck Institute for Chemical Ecology, D-07745 Jena, Germany,

²Department of Biochemistry, Max Planck Institute for Chemical Ecology, D-07745 Jena, Germany, and

³Department of Chemistry, W.M. Keck Institute for Proteomics Technology and Applications, George Washington University, Washington, DC 20052, USA

Received 22 December 2013; revised 21 December 2014; accepted 23 December 2014; published online 19 January 2015.

*For correspondence (e-mail gershenzon@ice.mpg.de).

[†]These authors contributed equally to this work.

[‡]Present address: Department of Biology, University of Utah, Salt Lake City, UT 84112, USA.

SUMMARY

The localization of metabolites on plant surfaces has been problematic because of the limitations of current methodologies. Attempts to localize glucosinolates, the sulfur-rich defense compounds of the order Brassicales, on leaf surfaces have given many contradictory results depending on the method employed. Here we developed a matrix-assisted laser desorption–ionization (MALDI) mass spectrometry protocol to detect surface glucosinolates on *Arabidopsis thaliana* leaves by applying the MALDI matrix through sublimation. Quantification was accomplished by spotting glucosinolate standards directly on the leaf surface. The *A. thaliana* leaf surface was found to contain approximately 15 nmol of total glucosinolate per leaf with about 50 pmol mm⁻² on abaxial (bottom) surfaces and 15–30 times less on adaxial (top) surfaces. Of the major compounds detected, 4-methylsulfinylbutylglucosinolate, indol-3-ylmethylglucosinolate, and 8-methylsulfinyloctylglucosinolate were also major components of the leaf interior, but the second most abundant glucosinolate on the surface, 4-methylthiobutylglucosinolate, was only a trace component of the interior. Distribution on the surface was relatively uniform in contrast to the interior, where glucosinolates were distributed more abundantly in the midrib and periphery than the rest of the leaf. These results were confirmed by two other mass spectrometry-based techniques, laser ablation electrospray ionization and liquid extraction surface analysis. The concentrations of glucosinolates on *A. thaliana* leaf surfaces were found to be sufficient to attract the specialist feeding lepidopterans *Plutella xylostella* and *Pieris rapae* for oviposition. The methods employed here should be easily applied to other plant species and metabolites.

Keywords: MALDI imaging, leaf surface, *Arabidopsis thaliana*, insect oviposition, *Plutella xylostella*, *Pieris rapae*, liquid extraction surface analysis, abaxial surface, adaxial surface, technical advance.

INTRODUCTION

Plant surfaces are known to play critical roles in the physiology of the plant and in resistance to biotic and abiotic stresses. They regulate the permeability of water and gases, restrict the loss and uptake of solutes, provide mechanical protection, shield against UV radiation, and protect against herbivores and pathogens (Müller and Riederer, 2005). In investigating many of these functions, it is

important to know which chemical compounds are actually present on the surface and which are in underlying cells. For example, UV-absorbing compounds on the surface can protect the entire organ (Kolb and Pfündel, 2005). Anti-herbivore defenses on the surface may deter insect herbivores before they even take a trial bite (Schoonhoven *et al.*, 2005). Insects and other arthropods may also

employ surface compounds for their own purposes in choosing suitable host plants for feeding and oviposition (Städler, 1991).

Despite many years of investigation, it has been difficult to establish procedures for unequivocally determining which compounds are on the plant surface and which are found only in underlying cells. Surface chemistry has been investigated by dipping leaves in solvents (Brooks *et al.*, 2003; Green *et al.*, 2003; Buschhaus and Jetter, 2012) and stripping the cuticle with gum arabic (Ensikat *et al.*, 2000; Jetter and Schäffer, 2001; Ringelmann *et al.*, 2009; Badenes-Pérez *et al.*, 2011), but the results have sometimes been contradictory. Mass spectrometry imaging with matrix-assisted laser desorption-ionization (MALDI) may be a feasible alternative since it has often been employed to determine the distribution of small molecules in biological samples with a high degree of sensitivity (Svatos, 2010; Kaspar *et al.*, 2011; Lee *et al.*, 2012). Since ionization is possible on close contact with the matrix molecule, restriction of the matrix to the surface could ensure that only surface substances are subject to analysis (Hankin *et al.*, 2007; Vrkoslav *et al.*, 2010). A problem in MALDI imaging is that measurements are usually made on a qualitative basis. It is difficult to add an internal standard to the sample without disturbing the original distribution of metabolites (Takai *et al.*, 2012). Yet accurate quantification is essential for surface analysis to compare the metabolite composition of different surfaces with each other and to that of the underlying tissue.

The surface localization of plant glucosinolates has been a controversial topic for many years. These sulfur-rich metabolites, found almost exclusively in families of the order Brassicales, are well-known plant defense compounds that are activated by glucohydrolase-mediated hydrolysis and rearrangement (Halkier and Gershenzon, 2006). Glucosinolates are frequently cited as key compounds for plants in deterring generalist insect herbivores and for specialist herbivores in choosing plants for feeding and oviposition (Mewis *et al.*, 2002; Miles *et al.*, 2005). Since insect behavioral choices are sometimes made after surface contact, glucosinolates have been sought on the surface. However, these efforts have yielded ambiguous results. Extracts obtained from various solvent dipping protocols were shown to contain glucosinolates (van Loon *et al.*, 1992; Renwick *et al.*, 1992; Hopkins *et al.*, 1997; Griffiths *et al.*, 2001; Marazzi *et al.*, 2004), but these studies were criticized because dipping also extracts glucosinolates from underlying tissues, possibly through stomatal openings (Reifenrath *et al.*, 2005; Städler and Reifenrath, 2009). Gum arabic peels were found to either contain glucosinolates (Badenes-Pérez *et al.*, 2011) or not (Reifenrath *et al.*, 2005; Städler and Reifenrath, 2009), but it is unclear how the peeling process affects glucosinolate recovery and hydrolysis.

Several years ago we employed MALDI mass spectrometry imaging to determine the spatial distribution of glucosinolates throughout the leaf tissue of *Arabidopsis thaliana* (Shroff *et al.*, 2008). We have now modified our procedures to detect only glucosinolates present on the leaf surface by applying the matrix through sublimation. The method was validated by employing two other surface analysis techniques, and put on a quantitative basis by spotting glucosinolate standards on the leaf. Approximately 1–5% of the total leaf glucosinolates were found to be present on the surface, and these were demonstrated to have biological significance by stimulating the oviposition of two specialist insect herbivores. The method should be applicable to determining whether many other classes of metabolites are localized on plant surfaces.

RESULTS

Leaf surface analysis via MALDI with matrix sublimation

To analyze the surface of *A. thaliana* leaves separately from the remainder of the leaf we developed a method for MALDI mass spectrometry in which the matrix 9-aminoacridine is deposited on the surface by sublimation. If the preparation were kept dry, we reasoned that the matrix would condense only on the surface and not penetrate the leaf. Thus only analytes from the surface would be ionized. The mass spectra recorded from both the abaxial (bottom) and adaxial (top) surfaces differed from each other and from the MALDI mass spectrum previously recorded from the whole leaf, as obtained by spraying the matrix in methanol solution (Shroff *et al.*, 2008). Compounds were identified by combining atmospheric pressure MALDI ionization with extensive collision-induced dissociation experiments and detection of products on an Orbitrap instrument. Spectra were compared with those of authentic standards and with data acquired previously (Shroff *et al.*, 2008).

The major glucosinolate detected previously from the whole leaf of *A. thaliana* was 4-methylsulfinylbutylglucosinolate (4MSOB, glucoraphanin) followed by indol-3-ylmethylglucosinolate (I3M, glucobrassicin), and 8-methylsulfinyloctylglucosinolate (8MSOO, glucohirsutin). In the surface analysis, these three glucosinolates were also detected but a fourth compound, 4-methylthiobutylglucosinolate (4MTB, glucoerucin), a putative biosynthetic precursor of 4MSOB, was one of the most abundant on the abaxial (lower) surface along with 4MSOB, followed by I3M and 8MSOO (Figure 1). The compound 4MTB was identified based on its tandem mass spectrometry (MS/MS) spectrum (m/z 420.0464, [M-H]⁻; major fragment at m/z 96.9614 [HSO₄]⁻) and database record (MassBank CE000483) (Scheubert *et al.*, 2012). On the adaxial surface, all four of these glucosinolates were also present, but in lower amounts, with 4MSOB being the most abundant. Across the surfaces, all glucosinolates were evenly

Figure 1. Negative mode matrix-assisted laser desorption-ionization time-of-flight mass spectra of the *Arabidopsis thaliana* leaf surface. Depicted are (a) adaxial (top) surface and (b) abaxial (bottom) surfaces on the same scale. Spectra were recorded after the matrix 9-aminoacridine was sublimed on 4-week-old leaves. The glucosinolate concentration is much higher on abaxial versus adaxial surfaces, and the composition is very different from that of total leaves measured after a matrix was deposited by spraying rather than sublimation (Shroff *et al.*, 2008). 4MTB, 4-methylthiobutylglucosinolate; 4MSOB, 4-methylsulfanylbutylglucosinolate; I3M, indol-3-ylmethylglucosinolate; 8MSOO, 8-methylsulfanyloctylglucosinolate.

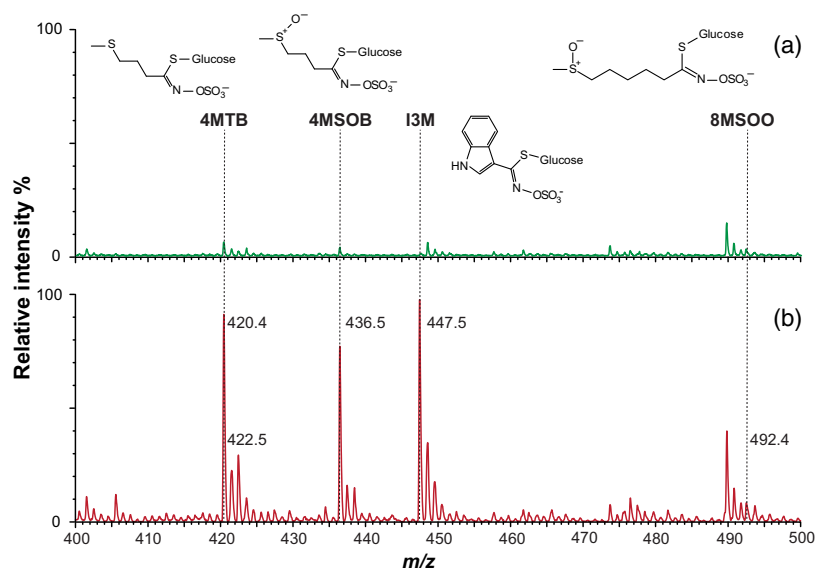
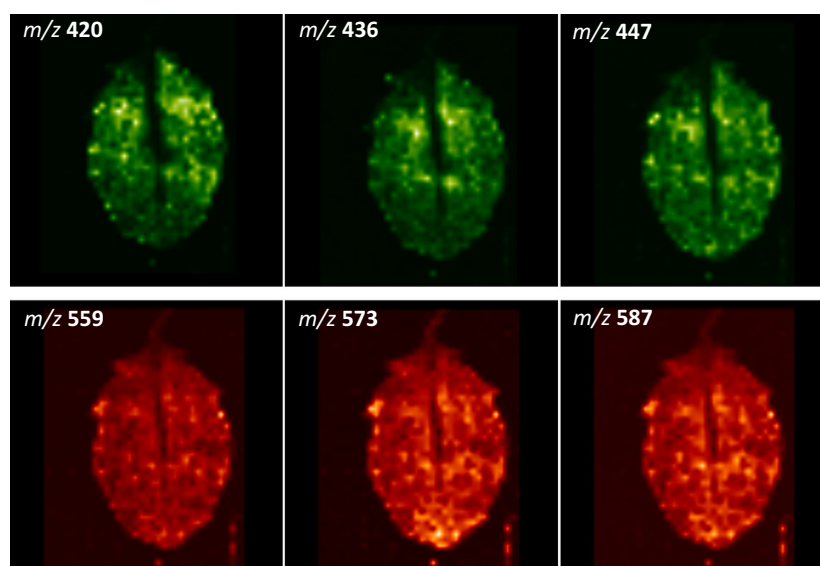


Figure 2. Matrix-assisted laser desorption-ionization time-of-flight mass spectrometry images of *Arabidopsis thaliana* leaf surfaces.

Images constructed for abundance of m/z 420 (4MTB, 4-methylthiobutylglucosinolate), 436 (4MSOB, 4-methylsulfanylbutylglucosinolate), 447 (I3M, indol-3-ylmethylglucosinolate), and m/z 559, 573, 587 for hydroxyl fatty acids from cutin. Surface glucosinolates do not show any pattern of localization on the edges of the leaf or around the midvein as previously demonstrated for total leaf glucosinolates (Shroff *et al.*, 2008).



distributed on the leaf except around the midrib where they were not present (Figure 2). Other compounds evident in the surface analysis (Table 1; Figure S1 in Supporting Information) included hydroxylated fatty acids and dimeric ester-linked fatty acid derivatives (Table 1) that are likely constituents of cutin, the abundant polyester polymer of leaf surfaces (Dominguez *et al.*, 2011). The results of the present MALDI method (deposition of matrix by sublimation) differed extensively from the results of the previous whole leaf analysis (deposition of matrix by spraying in methanol) in glucosinolate composition, glucosinolate distribution, and the presence of cutin fragments, suggesting that our present analysis was indeed restricted to actual surface constituents.

In a surface analysis, it should be possible to quantify mass spectrometric measurements by applying a standard directly to the surface, assuming an aqueous solution will not significantly penetrate the hydrophobic cuticle. A microarray spotter was therefore employed to deposit dilutions of a standard glucosinolate, 2-propenylglucosinolate (sinigrin, not found in *A. thaliana* Col-0), on the leaf surface (Figure 3). After sublimation with 9-aminoacridine and imaging of the standard spots by MALDI-time of flight (TOF), a plot of the amount of glucosinolate against signal intensity gave a linear range of 3.9–250 pmol mm⁻². This allowed quantification of the major glucosinolates on the abaxial surface of the leaf (Table 2; Figure S2). Measurements at 40 random points on each of five leaves gave an

Table 1 High-resolution mass spectrometric measurements of $[M-H]^-$ of oxygenated fatty acid derivatives from surface analysis. Data were obtained from 9-aminoacridine-sublimed *Arabidopsis thaliana* leaves prepared as for imaging experiments. Samples were measured on a MassTech AP-MALDI source connected to an LTQ-Orbitrap XL instrument operating at 70 000 mass resolution. The instrument was externally calibrated. The putative identifications are based on chemical analysis of isolated *A. thaliana* cuticle (Franke *et al.*, 2005)

$[M-H]^-$ m/z	Molecular formula	Δ (p.p.m.)	Putative identification
299.2591	$C_{18}H_{35}O_3$	0.99	18-Hydroxyoctadecanoic acid
489.4306	$C_{32}H_{57}O_3$	0.37	18-(Tetradecyloxy)octadecatrienoic acid
517.4644	$C_{34}H_{61}O_3$	2.85	18-(Hexadecyloxy)octadecatrienoic acid
531.4436	$C_{34}H_{59}O_4$	2.80	18-(Hexadecanoyloxy)octadecatrienoic acid
545.4955	$C_{36}H_{65}O_3$	2.67	18-(Octadecyloxy)octadecatrienoic acid
559.4738	$C_{36}H_{63}O_4$	1.71	18-(Octadecanoyloxy)octadecatrienoic acid
573.4552	$C_{36}H_{61}O_5$	3.87	18-(18-Hydroxyoctadecadienoyloxy)octadecadienoic acid
587.4689	$C_{37}H_{63}O_5$	1.85	Methyl 18-(18-hydroxyoctadecadienoyloxy)octadecadienoate

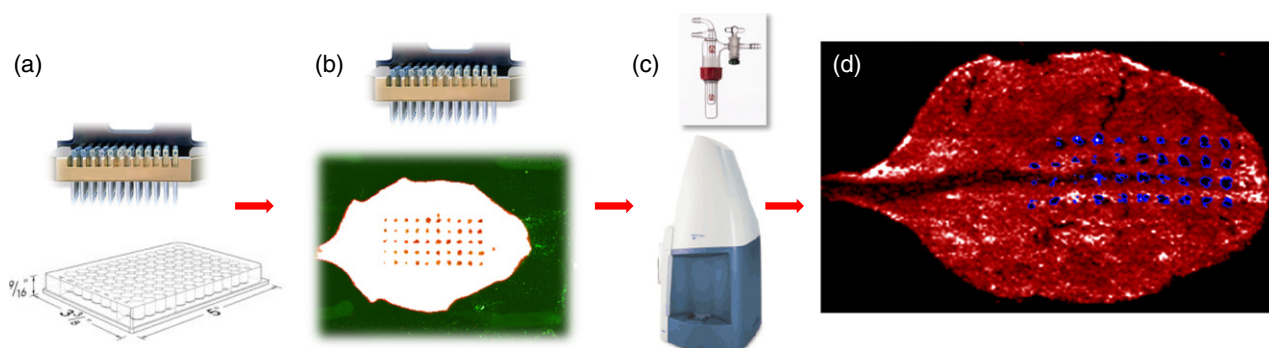


Figure 3. Procedure used for quantification of matrix-assisted laser desorption-ionization time-of-flight (MALDI-TOF) surface analysis of glucosinolates on *Arabidopsis thaliana* leaves.

- (a) A solution of internal standard (2-propenylglucosinolate) was mixed with fluorescent dye and transferred with a pin array spotter to the leaf surface.
 (b) The quality of spotting was checked by a fluorescence scan.
 (c) The spotted leaves were covered with 9-aminoacridine matrix by sublimation and measured by MALDI-TOF mass spectrometry in the negative mode.
 (d) Collected data were analyzed with BIOMAP software.

average density for total glucosinolates of just under 50 pmol mm^{-2} .

The glucosinolates on the adaxial surface were more difficult to quantify because it was not possible to reproducibly deposit the standard glucosinolate on the adaxial surface with the microarray spotter due to the presence of numerous trichomes. Quantities of glucosinolates on the adaxial surface were instead estimated from the calibration curves obtained from the abaxial surface using spectra run under the same conditions. The intensities of individual glucosinolate mass peaks from about 500 quantified spectra were averaged to obtain a calibration factor. The adaxial surface was found to have 15–30 times less total glucosinolate than the amount on the abaxial surface. The total amount on both surfaces represents about 1–5% (15 nmol) of the total glucosinolate content (350 nmol) of a typical *A. thaliana* rosette leaf (300 mm^2 , 20 mg dry weight) in the vegetative stage (Brown *et al.*, 2003).

Validation with other surface analysis methods

To confirm the findings of our surface analysis protocol, we also analyzed *A. thaliana* leaves by laser ablation

electrospray ionization (LAESI) mass spectrometry (Nemes and Vertes, 2010; Nemes *et al.*, 2010). In this method, an infrared laser is used to evaporate water molecules from the surface layer and the mixture of ionized and neutral metabolites formed is re-ionized by an electrospray source before detection by mass spectrometry. Analysis of detached *A. thaliana* leaves gave a very similar set of ions to that obtained from our MALDI measurements of a matrix-sublimed leaf with abundant 4MTB, 4MSOB, 13M, and 8MSOO (Figure 4). No cutin-associated hydroxy fatty acids were detected, but there was evidence for the flavonol diglycoside, kaempferol-3,7-*O*- α -L-dirhamnopyranoside (m/z 577) based on accurate mass measurements and collision-induced dissociation spectra (Figure S3) (Stracke *et al.*, 2007).

A second attempt to confirm our MALDI-TOF surface localization of glucosinolates employed liquid extraction surface analysis (LESA) using an automated, chip-based nanoelectrospray source for mass spectrometry. This technique deposits an aqueous solution with a small amount of organic solvent (20% propan-2-ol) on the leaf surface from a tip parked about 0.1 mm above the surface. The

Table 2 Quantification of glucosinolates on the abaxial surface of *Arabidopsis thaliana* leaves determined by quantitative matrix-assisted laser desorption-ionization time-of-flight mass spectrometry imaging experiments. An array of 2-propenylglucosinolate dilutions of different concentrations was deposited on the abaxial leaf surface and sublimed with a matrix of 9-aminoacridine. The linear fit for each leaf is indicated in the table footnotes

Leaf no.	Glucosinolate amounts (pmol mm ⁻²)		
	4MSOB	4MTB	I3M
1 ^a	21.2	16.2	11.9
2 ^b	22.4	16.5	14.7
3 ^c	20.9	15.2	11.7
4 ^d	23.5	18.7	13.6
5 ^e	20.7	13.5	10.3
Average	21.7	16.0	12.4
SD	1.0	1.6	1.4

4MSOB, 4-methylsulfinylbutylglucosinolate; 4MTB, 4-methylthiobutylglucosinolate; I3M, indol-3-ylmethylglucosinolate.

^a $y = 400.45055 + 1.92257x$.

^b $y = 406.1917 + 3.0974x$.

^c $y = 484.3944 + 2.45825x$.

^d $y = 477.31785 + 2.64378x$.

^e $y = 346.87517 + 2.98984x$.

droplet does not disperse, but remains on the waxy leaf surface and is subsequently aspirated back into the mass spectrometer after about 10 sec. The mass spectra obtained from the abaxial surface of *A. thaliana* were almost identical to those obtained from the MALDI analysis, displaying the presence of 4MTP, 4MSOB, I3M, and 8MSOO, as well as kaempferol-3,7-*O*- α -L-dirhamnopyranoside (Figure 5). Analysis of the adaxial leaf surface showed less intense signals for glucosinolates, but the kaempferol glycoside was dominant.

To compare glucosinolate content of the surface and the interior of the leaf, the deposition tip was set lower to

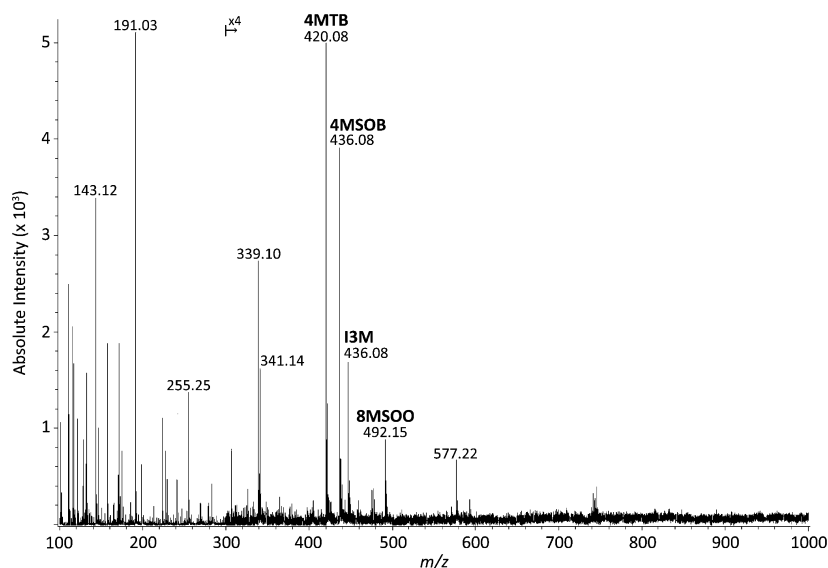
damage the leaf and place the droplet within leaf tissue. Using an internal standard (2-propenylglucosinolate) to correct for signal inhomogeneity, the levels of two glucosinolates, 4MSOB and I3M, were quantified on both the surface and within the leaf (Figure S4). The level of glucosinolates in the leaf tissue was 98 times (4MSOB) and 87 times (I3M) higher than on the surface, which compares well with the estimate from MALDI analysis of 1–5% of total leaf glucosinolates on the surface.

Biological significance of surface glucosinolates for insect oviposition

The importance of surface glucosinolates as cues for specialist herbivores was investigated in oviposition assays using *Plutella xylostella* and *Pieris rapae*, two lepidopteran specialists on Brassicaceae species that have been reported to use glucosinolates as oviposition stimulants (Renwick *et al.*, 1992; Hughes *et al.*, 1997). Of the glucosinolates found on the surface of *A. thaliana*, 4MTB, 4MSOB, and I3M were tested individually and as mixtures in concentrations resembling those of either the adaxial and abaxial surface. Individual compounds were tested with *P. xylostella* and mixtures with both *P. xylostella* and *P. rapae*.

In tests with individual glucosinolates, *P. xylostella* oviposition occurred predominantly on glucosinolate-coated Parafilm versus solvent controls without glucosinolates. This choice was significant for 4MTB and I3M, but not for 4MSOB (Figure 6). For 4MTB and I3M, the abaxial concentrations (over 20 and 25 times greater, respectively, than the adaxial concentrations) received proportionally more eggs than the adaxial concentration (Figure 6 within rows). While 4MSOB was not attractive at the tested concentrations, 4MTB and I3M were almost equally attractive for ovipositing female *P. xylostella*.

Figure 4. Mass spectrum obtained from analysis of the *Arabidopsis thaliana* abaxial surface as imaged with laser ablation electrospray ionization mass spectrometry. A quantitative time-of-flight instrument was used. The major glucosinolates detected and their relative abundance were similar to that observed in matrix-assisted laser desorption-ionization time-of-flight analyses of the abaxial surface.



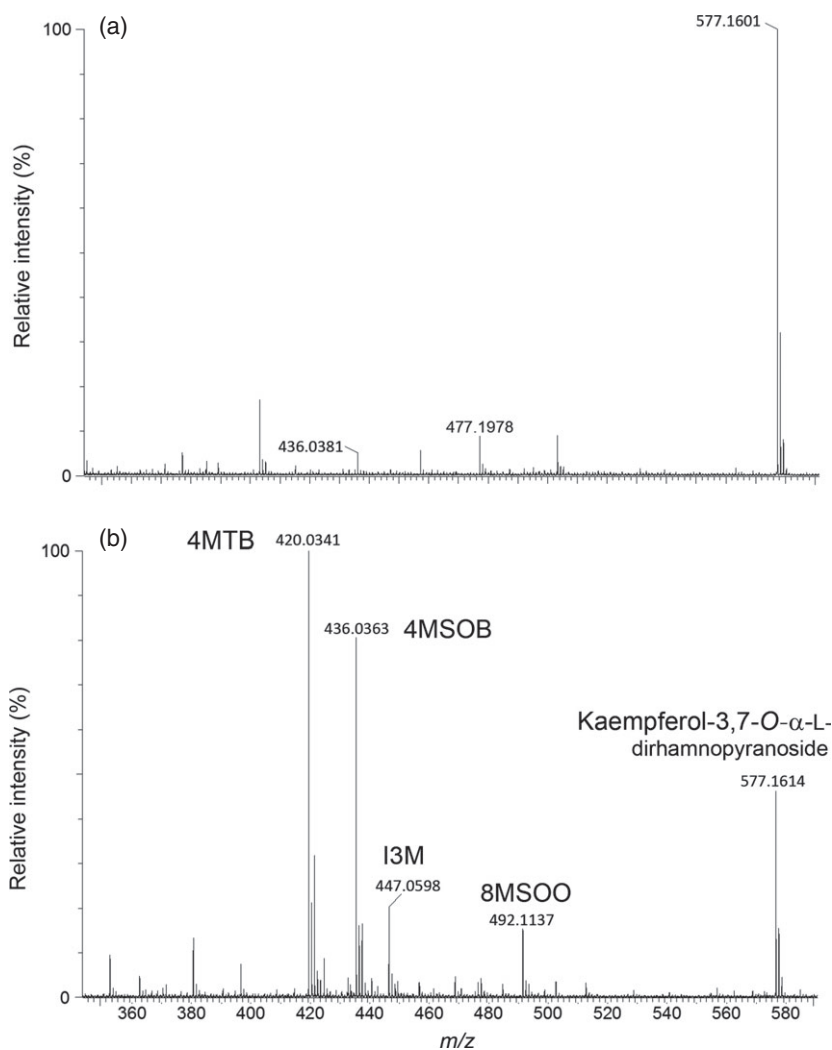


Figure 5. Mass spectrum obtained from analysis of *Arabidopsis thaliana* leaf surfaces by LESA. Depicted are adaxial (a) and abaxial (b) leaf surfaces of *A. thaliana* by LESA using a nano-electrospray source interfaced with a Synapt high-resolution mass spectrometer. A droplet of an aqueous solution containing 0.1% ammonium hydroxide and 20% propan-2-ol was deposited on each surface for 20 sec and aspirated into the source. The major glucosinolates detected and their relative abundance were similar to that observed in matrix-assisted laser desorption-ionization time-of-flight analyses of the surface.

When the glucosinolates were offered as mixtures, the two species reacted differently. Female *P. rapae* deposited significantly more eggs on the mixtures than on the solvent controls (Figure 7a,b), with the effect being more pronounced for the mixture mimicking the concentrations of the bottom surface of the leaf (Figure 7b). Moreover, when comparing the glucosinolate mixtures of the two surfaces against each other, the abaxial mixture received significantly more eggs (Figure 7c). Under similar experimental conditions, female *P. xylostella* did not show a significant preference for either natural mixture versus the control (Figure S5A). However, this species tended to choose the adaxial mixture in preference to the solvent control ($P = 0.07$).

The glucosinolates 4MTB and I3M may have special importance in leaf surface recognition since 4MTB is relatively much more abundant on the surface than in the leaf interior while I3M is characteristic of the periphery of the leaf (Shroff *et al.*, 2008). When the concentrations of 4MTB

and I3M were raised significantly above natural levels (approximately two- and fourfold, respectively) while maintaining the original 4MSOB concentration, female *P. xylostella* showed oviposition preferences comparable to female *P. rapae* choosing the glucosinolate mixtures over the controls (Figure S5B). Whether these results were due to the overall higher glucosinolate concentration or the altered relative proportions of the individual glucosinolates in the mixture was not determined.

DISCUSSION

Imaging by MALDI mass spectrometry has been used to determine the fine-scale distribution of metabolites in many types of plant and animal tissues. Here we restricted matrix application to the surface of *A. thaliana*, and were thus able to analyze the content of the surface without interference from underlying tissues. The major glucosinolates on *A. thaliana* leaf surfaces were found to be 4MSOB and 4MTB followed by I3M and 8MSOO, while in the

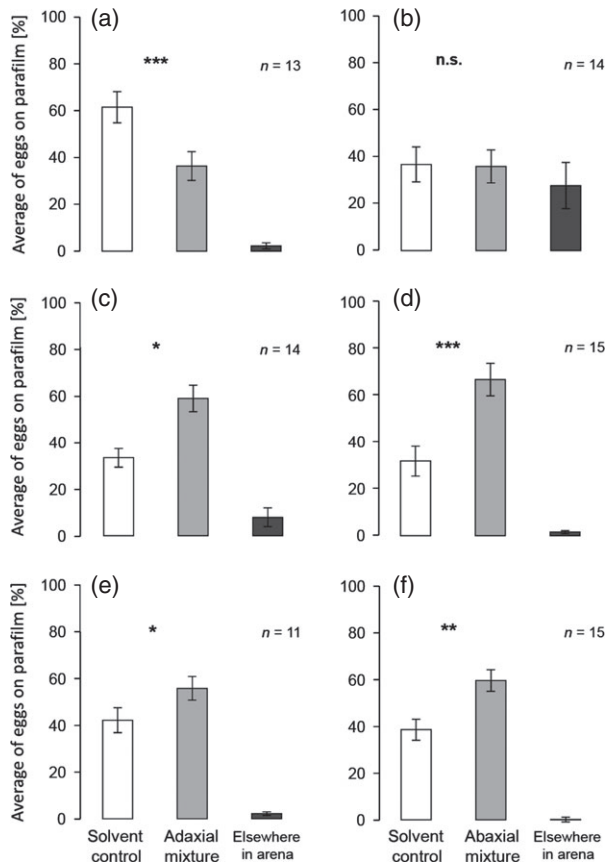


Figure 6. Distribution of *Plutella xylostella* eggs in an oviposition choice assay using individual purified glucosinolates.

Glucosinolates were applied in methanol to a piece of Parafilm and tested against methanol controls. Compounds tested: (a, b) 4-methylsulfinylbutylglucosinolate (4MSOB); (c, d) 4-methylthiobutylglucosinolate (4MTB); (e, f) indol-3-ylmethylglucosinolate (I3M). Compounds were tested at concentrations characteristic of the adaxial (top) (a, c, e) and the abaxial (bottom) (b, d, f) surface. For 4MTB and I3M, moths oviposited significantly more often on the glucosinolate-coated strip. Statistical analysis by ANOVA with significance indicated by: * $P < 0.05$, ** $P < 0.01$, *** $P < 0.001$.

whole leaf 4MSOB is dominant followed by I3M and 8MSOO, but little 4MTB (Brown *et al.*, 2003; Shroff *et al.*, 2008). By spotting known amounts of glucosinolates on the leaf surface, we were able to quantify the total surface glucosinolate pool as containing approximately 50 pmol mm^{-2} on the abaxial (bottom) surface and about 3 pmol mm^{-2} on the adaxial (top) surface, representing about 1–5% of the total glucosinolate content of a typical rosette stage *A. thaliana* leaf (Brown *et al.*, 2003). It has usually not been possible to carry out MALDI imaging in such a quantitative manner. However, the ease in reproducibly spotting a glucosinolate standard on the leaf, and the availability of a pure glucosinolate not present in *A. thaliana*, facilitated a quantitative approach.

The results of MALDI imaging were confirmed by two other mass spectrometry-based surface analysis techniques, LAESI (Nemes and Vertes, 2007) and LESA (Kertesz and Van Berkel, 2009), with the latter distinguishing between the low leaf surface concentrations of glucosinolates and the much higher internal ones. Like MALDI imaging, these techniques also have promise in analyzing plant surfaces but require special trial and error adjustment for each species and organ to be sure that the analytes detected come only from the surface and not the underlying tissue. The spatial resolution of LESA is limited to areas greater than 1 mm^2 . Moreover, the time and cost of the technique prevent it from being more widely employed. It seems that LAESI is an ideal method for surface as well as full three-dimensional imaging (Nemes *et al.*, 2009). However, as presently employed it is unsuitable for leaf tissue of low tensile strength, such as that of *A. thaliana*. The utilization of LAESI for three dimensional imaging of this tissue will require further refinement of depth resolution, particularly by carefully controlling the energy and stability of the incident mid-infrared laser pulses during ablation.

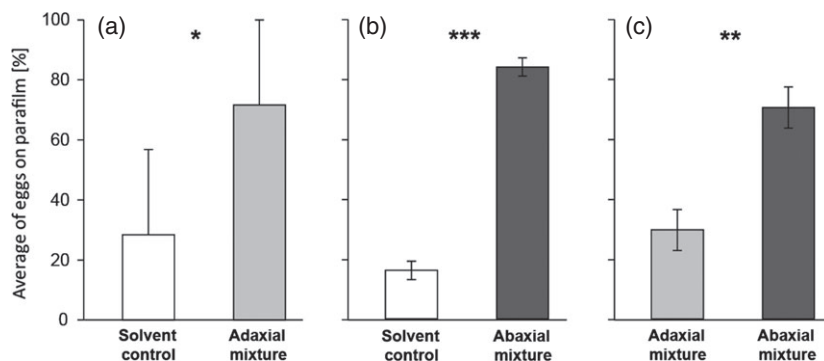


Figure 7. Distribution of *Pieris rapae* eggs in an oviposition choice assays using glucosinolate mixtures.

Mixtures were prepared from purified 4-methylthiobutylglucosinolate (4MTB), 4-methylsulfinylbutylglucosinolate (4MSOB), and indol-3-ylmethylglucosinolate (I3M) at concentrations found on either the abaxial or adaxial leaf surface. Compounds were applied to pieces of Parafilm in methanol with controls receiving pure methanol. Separate choice assays were made comparing either an abaxial or an adaxial concentration of the glucosinolate mixture with a solvent control, (a) and (b), or with each other (c). Mixtures of glucosinolates attracted more oviposition than controls, and the abaxial glucosinolate concentration received more oviposition than the adaxial concentration. $n = 3$ for all treatments. Statistical analysis by ANOVA with significance indicated by: * $P < 0.05$, ** $P < 0.01$, *** $P < 0.001$.

Previous attempts to determine the levels of glucosinolates on leaf surfaces have met with mixed results. A number of studies have found evidence for surface glucosinolates by dipping leaves in solvents, such as chloroform or dichloromethane followed by methanol (Städler and Roessingh, 1991; van Loon *et al.*, 1992; Renwick *et al.*, 1992; Hopkins *et al.*, 1997; Griffiths *et al.*, 2001) or chloroform:methanol:water (2:1:1) (Reifenrath *et al.*, 2005; Städler and Reifenrath, 2009). However, glucosinolates found in such extracts could have come from inside the leaf, possibly via stomata since stomatal opening has been directly correlated with an increase in the glucosinolate content of extracts obtained by dipping (Reifenrath *et al.*, 2005). Other authors employed gum arabic peelings detecting glucosinolates on the leaf surfaces of *Barbarea* sp. (Badenes-Pérez *et al.*, 2011), but not on *Brassica napus* and *Nasturtium officinale* (Reifenrath *et al.*, 2005; Badenes-Pérez *et al.*, 2011). The level of glucosinolates in such peels may be in the nanogram range, below the detection levels of many HPLC systems. Moreover, peeling could lead to leaf damage that promotes myrosinase-mediated glucosinolate hydrolysis, thus reducing the apparent glucosinolate content even further.

Our MALDI imaging protocol avoids leaf damage and restricts detection solely to analytes deposited on the surface since the matrix is applied by sublimation. Surface analysis might also be carried out by infrared microscopy (Schmitt *et al.*, 1997; Walter *et al.*, 2010), but it would be difficult to find an absorption band that would distinguish glucosinolates from other surface constituents. Raman spectroscopy might also be problematic because of its lack of sensitivity to low concentrations. Matrix-free laser desorption ionization mass spectrometry (i.e. MALDI without a matrix; Hölscher *et al.*, 2009) might also be attempted for glucosinolates, but the lack of strong UV absorption of most compounds of this class, except for the indolic glucosinolates, is likely to hinder detection. Typical MALDI imaging for glucosinolates was employed recently on *A. thaliana* floral organs along with energy dispersion X-ray analysis for sulfur detection (Sarsby *et al.*, 2012). These showed convincingly that glucosinolates in the sepal were present in surface cell layers, but the surface itself was not examined.

The composition and distribution of glucosinolates on the surface of *A. thaliana* leaves differs from that in the leaf interior in several ways. [As a measure of interior glucosinolates we rely on the results of our earlier MALDI imaging protocol (Shroff *et al.*, 2008). Although total leaf glucosinolates (surface + interior) were measured in this protocol, the data reflect the interior pools since surface glucosinolates make up only a small proportion of the total.] A first major difference is that the surface is enriched in 4MTB. Compared with 4MSOB, the major glucosinolate of *A. thaliana* Col-0 ecotype, 4MTB, has a less polar side chain and

may have greater solubility in the surface wax. Interestingly, a recent survey of the glucosinolates of *A. thaliana* floral tissues revealed that the siliques are enriched in 4-benzoyloxybutylglucosinolate (Sarsby *et al.*, 2012), another glucosinolate with a less polar side chain that may be more suitable for storage in the low-water environment of the dried fruit and seed.

Second, the distribution of glucosinolates on the surface, with the exception of the midrib, is relatively uniform. This contrasts with the distribution in the interior of the leaf where glucosinolates were found to be much more abundant in the midrib and along the periphery of the leaf than in the inner lamina (Shroff *et al.*, 2008). The uniform distribution does not provide any hints about whether glucosinolate transport to the surface is associated with specific locations, such as stomata, or occurs in all epidermal cells. However, the resolution of our analysis (50 µm) may not have permitted us to distinguish such patterns.

Third, the glucosinolate content of the upper (adaxial) and lower (abaxial) leaf surfaces differ significantly, with the lower having a concentration that is 15–30 times higher. This trend is also evident in previous work using solvent dips or leaf peels which report that the lower surface has two to eight times (*Barbarea*, sp.; Badenes-Pérez *et al.*, 2011), up to two and a half times (*B. napus*; Reifenrath *et al.*, 2005), or at least three times (*N. officinale*; Reifenrath *et al.*, 2005) more glucosinolate than the upper surface. This greater amount on the lower surface has been suggested to be a consequence of the greater number of stomata on this surface, assuming glucosinolate transport to the surface is associated with stomata (Reifenrath *et al.*, 2005; Badenes-Pérez *et al.*, 2011). It may also arise from greater selection for glucosinolate defenses on the lower surface due to increased herbivore or pathogen pressure on this side.

At least some of the glucosinolates detected on the leaf surface of *A. thaliana* may be located in trichomes. A recent study reported that isolated *A. thaliana* trichomes contain 4MSOB, 8MSOO, I3M, and other indolic glucosinolates (Frerigmann *et al.*, 2012). This list includes the major glucosinolates we found on the whole surface by MALDI mass spectrometry, except for 4MTB which was not detected. Glucosinolates in the trichomes were reported at levels 100 times less than in the leaves, which is in the range that we found for surface glucosinolates.

To determine if the concentrations of glucosinolates found on leaf surfaces are biologically significant, we employed them in behavioral bioassays with two lepidopteran specialists of the Brassicaceae that are known to employ glucosinolates as oviposition stimulants, the diamondback moth (*P. xylostella*) and the small cabbage white (*P. rapae*) (Reed *et al.*, 1989; Traynier and Truscott, 1991; Renwick *et al.*, 1992; Huang *et al.*, 1994; Huang and Renwick, 1994; Hughes *et al.*, 1997; Renwick *et al.*, 2006;

Sun *et al.*, 2009; Badenes-Pérez *et al.*, 2011). In assays with the individual compounds, female *P. xylostella* were more attracted to I3M and 4MTB for oviposition than to 4MSOB, which was not significantly more attractive than the control and may even have had a deterrent effect (Figure 7a). These results parallel those of previous studies on the attraction of glucosinolates to ovipositing *P. xylostella* but the concentrations used here were significantly lower (Reed *et al.*, 1989; Sun *et al.*, 2009; Badenes-Pérez *et al.*, 2011). As a specialist feeder on Brassicaceae that is not affected by glucosinolates in its diet (Müller *et al.*, 2010), it is not surprising that *P. xylostella* is attracted for egg laying by characteristic compounds of its host plants. This species also has metabolic adaptations to glucosinolates, desulfating them on ingestion (Ratzka *et al.*, 2002). Desulfated glucosinolates are no longer substrates for myrosinase-catalyzed hydrolysis and thus do not lead to toxic products. In comparing the attraction of various products, Sun *et al.* (2009) clearly demonstrated that indolic glucosinolates were more attractive than aliphatic glucosinolates such as 4MSOB. Moreover, among indolic glucosinolates, such as I3M, intact compounds were more attractive than hydrolysis products, although for aliphatic glucosinolates the reverse was true (Renwick *et al.*, 2006; Sun *et al.*, 2009).

Interestingly, the results from the assays testing intact glucosinolates as mixtures of the three major compounds in differing concentrations suggest that the two lepidopterans react differently to surface glucosinolates. For *P. rapae*, the mixtures were oviposition stimulants at concentrations approximating those found naturally on the leaf surface. Concentrations similar to those on the lower surface (approximately 50 pmol mm⁻²) were more attractive than concentrations similar to those on the upper surface (approximately 3 pmol mm⁻²). For *P. xylostella*, neither of the tested mixtures was significantly attractive (Figure S5A), although there was a trend towards attraction by the mixture approximating the lower surface. When the glucosinolate mixture was tested after 4MTB and I3M concentrations were increased approximately two and four times, respectively, while 4MSOB was held constant, *P. xylostella* was significantly more attracted to glucosinolates than controls for oviposition (Figure S5B) and preferred the abaxial over the adaxial concentration. The result may be due to the overall higher concentration of glucosinolates employed in this second set of mixtures or the change in relative proportions of the individual compounds in the mixture. Taken together with the results from the tests with individual glucosinolates, this suggests that 4MSOB may have a deterrent effect on oviposition by *P. xylostella* that is abolished when more attractive glucosinolates are present at higher concentrations.

The importance of intact glucosinolates as oviposition stimulants for *P. xylostella* and *P. rapae* raises questions

about where insects encounter them in the course of oviposition on the leaf surface. Since any leaf damage would normally trigger the formation of hydrolysis products, intact glucosinolates would have to be exposed on the surface or located internally in a site far from myrosinase in order to be used as an oviposition cue. Our demonstration of intact glucosinolates on the *A. thaliana* leaf surface supports the first possibility. However, for *P. rapae* and other insect herbivores, it has sometimes been suggested that glucosinolate perception requires scratching the leaf surface to expose internal glucosinolates or to release hydrolysis products (Renwick *et al.*, 2006; Städler and Reifenthat, 2009). In contrast, our data suggest that detection of intact glucosinolates by *P. xylostella* and *P. rapae* is possible directly upon landing on the surface via antennal or tarsal contact receptors.

From the perspective of the plant, the presence of glucosinolates on the leaf surface must bring benefits to offset any promotion of herbivore oviposition. For example, these substances could serve as a first line of defense against pathogens. Being close to the ground, *A. thaliana* rosette leaves may be especially susceptible to colonization by soil-borne pathogens and require effective defenses. Among the glucosinolates found on the surface, I3M especially is known to have antipathogen effects because of the direct activity of its hydrolysis products (Brader *et al.*, 2001) and the antifungal role of other breakdown products (Bednarek *et al.*, 2009; Clay *et al.*, 2009; Hiruna *et al.*, 2010). The absence of glucosinolates on the midvein may be a consequence of the fact that this tissue is too tough for fungal penetration regardless of the presence of chemical defenses on the leaf surface.

EXPERIMENTAL PROCEDURES

Plant material and growth conditions

Arabidopsis thaliana Col-0 plants were grown under the same cultivation conditions as described previously (Shroff *et al.*, 2008). Detached rosette leaves from 4-week-old plants were used in all experiments.

Insects and culture conditions

Plutella xylostella larvae were raised from eggs from a colony maintained at the Max Planck Institute for Chemical Ecology, Jena by L. Knolhoff and D. G. Heckel. They were reared on an artificial diet (Shelton *et al.*, 1991) at 21°C and 50% humidity with a photoperiod of 12 h light and 12 h darkness. Pupae were collected individually into lidded 10 ml plastic tubes and kept under the above described conditions until eclosion, after which moths were sexed and randomly assigned into breeding couples for oviposition assays.

Pieris rapae eggs were purchased from the Entomological Laboratory at Wageningen University. Larvae were kept in a mesh cage (45 × 90 × 45 cm) on 6–8-week-old *Brassica oleracea* var *gemmifera* plants at 21°C and 70% humidity with a photoperiod of 12 h

light and 12 h darkness. Pupae were mounted individually on 1 × 2 cm pieces of carton and kept in lidded 36-ml clear Solo cups (Market Grounds GmbH, <http://www.market-grounds.com>) until butterfly emergence. Every day, newly emerged butterflies were placed in mesh cages (46 × 46 × 46 cm) with a 10% aqueous honey solution and allowed to mate. After 4 days, female butterflies were randomly assigned to a glucosinolate treatment in the oviposition assays.

Chemicals

9-Aminoacridine base was prepared as described earlier (Shroff *et al.*, 2008) while all other solvents and chemicals were used as-delivered. Intact glucosinolates were obtained from seeds of various species of the Brassicaceae (I3M from *Isatis tinctoria*; 4MTB from *Eruca sativa*; and 4MSOB from *B. oleracea* var. *italica*) according to previously described procedures (Badenes-Pérez *et al.*, 2011). For the oviposition assays, the intact glucosinolates were resuspended in methanol.

Matrix coating of leaves by sublimation

Leaves were detached from 4-week-old *A. thaliana* plants, attached on a glass microscope slide (four leaves on one slide) with double-sided carbon-conductive adhesive tape, and the slide placed on a metallic MALDI plate with either the abaxial (bottom) or adaxial (top) side facing the observer. The MALDI plate was inserted in a sublimation chamber and 9-aminoacridine crystals (typically about 1 g) were sublimated on the leaves for 10 min (oil bath temperature 170°C; 2×10^{-3} mbar). The inner part of the sublimation chamber where the plate with the leaf was attached was cooled using cold water for faster matrix crystallization and to maintain a smaller crystal size. After sublimation, the sample was cooled to 25°C before imaging. Other procedures, including external calibration with polyethylene glycol oligomers added to the leaf after sublimation, were performed as described (Svatoš and Mock, 2013).

MALDI-TOF mass spectrometry

A MALDI-TOF micro MX mass spectrometer (Waters, <http://www.waters.com/>) fitted with a nitrogen laser (337 nm, 4 ns laser pulse duration, 20 Hz and 150 µJ per pulse) was used in the reflectron mode and negative ion polarity mode for data acquisition using MASSLYNX version 4.0 software (www.waters.com/en-US/MassLynx-Mass-Spectrometry-Software). The chemical identities of the respective glucosinolates were confirmed by comparing collision-induced dissociation (CID) spectra of analyte peaks with CID spectra obtained for synthetic standards. The CID measurements were made on an LTQ ion trap mass spectrometer (ThermoFisher, <http://www.thermofisher.com/>) fitted with an atmospheric pressure MALDI source (MassTech, <http://www.apmaldi.com>; solid state Nd-YAG UV laser) running TARGET 6 (MassTech) software for data acquisition (Shroff *et al.*, 2008).

Imaging

The coordinates for imaging were pre-defined using proprietary software with a setting of 50 µm for spatial resolution. Each MASSLYNX raw data file was then converted into a format suitable for further evaluation using the MALDI IMAGING-CONVERTER (Waters) software. The converted data files were then imported into BIOMAP (3.8.0; Novartis, <http://www.novartis.com/>) for image visualization and processing. The spectra were baseline-corrected and smoothed in BIOMAP. Ion intensity maps or images were constructed using a mass window of 0.25 Da for all analyte peaks

corresponding to glucosinolates. Each ion-intensity map was normalized against the intensity of the matrix ion (193.07; [M-H]⁻).

Quantification

The standard 2-propenylglucosinolate (sinigrin) was serially diluted in water to give concentrations ranging from 500 pmol per 1.8 nl to 976 fmol per 1.8 nl. All dilutions were spiked with water-soluble fluorescent Cy3 dye (0.5 fmol per 1.8 nl) to make them visible. Five spots for each concentration were then deposited on each leaf using a microarray pin spotter (OmniGrid Microarrayer; GeneMachines). Each spot was about 250 µm in diameter and adjacent spots were spaced 500 µm apart. After spotting, the leaves were dried at 20°C for 2 h. Optical images of the leaves were made using a ScannArray-3000 (GSI Lumonics, <http://www.gsig.com/>) to assess spotting efficiency and whether the spotter point damaged the leaf surface, but no damage was noted based on the absence of chlorophyll autofluorescence associated with the spots. The spotted leaves were then coated with 9-aminoacridine as described above. The spotted leaf was imaged by MALDI-TOF mass spectrometry at high spatial resolution (50 µm) with at least 20 data points per spot to control for local surface unevenness.

Data analysis

Quantification of the respective glucosinolates was carried out using the BIOMAP software. After the actual size of leaves was calculated from pixel size, circular areas corresponding to a diameter of 4.9 mm² were made on each image around the 40 spots of 2-propenylglucosinolate made by the microarray pin spotter. The integrated signal intensities for each spot were determined and a mean value for integrated signal intensity was calculated for each concentration on each leaf by averaging the signal intensities for the five replicates. Finally, a calibration curve was generated with the amounts of spotted 2-propenylglucosinolate plotted against the mean integrated signal intensity. The same procedure was repeated for each of the five replicate leaves and the results combined to give a single average calibration curve ($r^2 = 0.95$, $P < 0.001$). Each of the major glucosinolates was quantified by taking its signal intensity at 40 random points on each leaf surface (circles of diameter 4.9 mm²). The 2-propenylglucosinolate calibration curve was then employed to obtain the amount of glucosinolate present. All statistics were performed using ORIGIN version 8.0 software (<http://www.originlab.com>).

Laser ablation electrospray ionization mass spectrometry

See Method S1 in the Supporting Information.

Liquid extraction surface analysis

See Method S2 in the Supporting Information.

Oviposition assays

Glucosinolates were tested individually against a solvent control in concentrations in the range of those found either on the upper leaf surface (adaxial side) or the lower surface (abaxial side). Tests were also carried out in mixtures mimicking the concentration on either the adaxial or abaxial side of the leaf. In this approach, both an adaxial and an abaxial mixture were tested against a solvent control and then tested against each other. For the abaxial surface, concentrations used were: I3M, 9 pmol mm⁻²; 4MTB, 17 pmol mm⁻²; 4MSOB, 22 pmol mm⁻². For the adaxial surface, concentrations were 14–30 times lower: I3M, 0.3 pmol mm⁻²; 4MTB,

0.9 pmol mm⁻²; 4MSOB, 1.5 pmol mm⁻². To compare the attractiveness of the glucosinolate mixture, the three glucosinolates were mixed at the respective concentrations. In a second experiment, the concentrations of 4MTB and I3M were raised above their natural levels to 30 and 39 pmol mm⁻², respectively, to test the effect of these higher concentrations on *P. xylostella* oviposition.

Plutella xylostella

Oviposition assays were conducted in 80 ml ice-cream cups, capped with transparent plastic lids with a meshed hole for air exchange. Glucosinolates were presented on pieces of Parafilm (2.5 × 2.5 cm) to mimic surface waxes because of the previously reported synergistic attraction of glucosinolates and surface waxes in promoting *P. xylostella* oviposition (Spencer *et al.*, 1999). Parafilm slices were etched with a toothpick to provide an uneven surface and stapled onto opposite sides of a cup. Each male–female pair was assigned to one of the treatments ($n = 15$). Mating and oviposition were allowed to proceed for 48 h under the light and humidity regime described above. A 10% honey solution was provided as the food source. After 48 h, the cups, including moths and eggs, were moved to a freezer at -20°C until the eggs were counted under a stereo microscope.

Pairs producing fewer than 20 eggs were discarded from the analysis. Results were expressed as mean percentage of eggs laid in each location per pair. For statistical analysis, data were arcsine-square transformed and analyzed using an ANOVA in R (<http://www.R-project.org>).

Pieris rapae

Oviposition assays were conducted in 9-L clear plastic boxes closed with meshed lids. Glucosinolates were presented on round pieces of Parafilm (diameter 3 cm) mounted onto Parafilm-covered Eppendorf dishes (diameter 5.3 cm). Each female was assigned to one of the treatments using the glucosinolate mixes ($n = 3$). Oviposition was allowed to proceed for 48 h under the light and humidity regime described above. A 10% aqueous honey solution was provided as the food source. After 48 h, the boxes were moved to a freezer at -20°C until the eggs were counted.

Pairs producing fewer than 15 eggs were discarded from the analysis. Results were expressed as mean percentage of eggs laid in each location per female. For statistical analysis, data were arcsine-square transformed and analyzed using an ANOVA in R (<http://www.R-project.org>).

ACKNOWLEDGEMENTS

We thank Lisa Knolhoff and David Heckel for the diamondback moth larvae and the Max Planck Society and the International Max Planck Research School in Jena for financial support. Two of the authors (PN and AV) acknowledge the financial support from the Division of Chemical Sciences, Geosciences, and Biosciences, Office of Basic Energy Sciences of the US Department of Energy (Grant DE-FG02-01ER15129) that supported the LAESI portion of this study.

SUPPORTING INFORMATION

Additional Supporting Information may be found in the online version of this article.

Figure S1. Negative-mode matrix-assisted laser desorption/ionization time-of-flight mass spectrometry spectrum of an *Arabidopsis thaliana* leaf surface showing extended mass range, m/z 400–600.

Figure S2. Calibration curve of the internal standard used to quantify glucosinolates on *Arabidopsis thaliana* leaf surfaces.

Figure S3. Identification of a flavonol diglycoside based on liquid extraction surface analysis with a fixed precursor ion scan for m/z 577.

Figure S4. Comparison of the glucosinolate content of the leaf surface versus the leaf interior via liquid extraction surface analysis.

Figure S5. Distribution of *Plutella xylostella* eggs in an oviposition choice assay using glucosinolate mixtures.

Method S1. Laser ablation electrospray ionization mass spectrometry.

Method S2. Liquid extraction surface analysis.

REFERENCES

- Badenes-Pérez, F.R., Reichelt, M., Gershenzon, J. and Heckel, D.G. (2011) Phylloplane location of glucosinolates in *Barbarea* spp. (Brassicaceae) and misleading assessment of host suitability by a specialist herbivore. *New Phytol.* **189**, 549–556.
- Bednarek, P., Pislewska-Bednarek, M., Svatos, A. *et al.* (2009) A glucosinolate metabolism pathway in living plant cells mediates broad-spectrum antifungal defense. *Science*, **323**, 101–106.
- Brader, G., Tas, E. and Palva, E.T. (2001) Jamsionate-dependent induction of indole glucosinolates in *Arabidopsis* by culture filtrates of the non-specific pathogen *Erwinia carotovora*. *Plant Physiol.* **126**, 849–860.
- Brooks, J.S., Williams, E.H. and Feeny, P. (2003) Quantification of contact oviposition stimulants for black swallowtail butterfly, *Papilio polyxenes*, on the leaf surfaces of wild carrot, *Daucus carota*. *J. Chem. Ecol.* **22**, 2341–2357.
- Brown, P.D., Tokuhisa, J.G., Reichelt, M. and Gershenzon, J. (2003) Variation of glucosinolate accumulation among different organs and developmental stages of *Arabidopsis thaliana*. *Phytochemistry*, **62**, 471–481.
- Buschhaus, C. and Jetter, R. (2012) Composition and physiological function of the wax layers coating *Arabidopsis* leaves: β -amyryn negatively affects the intracuticular water barrier. *Plant Physiol.* **120**, 1160–1169.
- Clay, N.K., Adio, A.M., Denoux, C., Jander, G. and Ausubel, F.M. (2009) Glucosinolate metabolites required for an *Arabidopsis* innate immune response. *Science*, **323**, 95–101.
- Dominguez, E., Heredia-Guerrero, J.A. and Heredia, A. (2011) The biophysical design of plant cuticles: an overview. *New Phytol.* **189**, 938–949.
- Enskat, H.J., Neinhuis, C. and Barthlott, W. (2000) Direct access to plant epicuticular wax crystals by a new mechanical isolation method. *Int. J. Plant Sci.* **161**, 143–148.
- Franke, R., Briesen, I., Wojciechowski, T., Faust, A., Yephremov, A., Nawrath, C. and Schreiber, L. (2005) Apoplastic polyesters in *Arabidopsis* surface tissues – A typical suberin and a particular cutin. *Phytochemistry*, **66**, 2643–2658.
- Frerigmann, H., Böttcher, C., Baatout, D. and Gigolashvili, T. (2012) Glucosinolates are produced in trichomes of *Arabidopsis thaliana*. *Front. Plant Sci.* **3**, 242.
- Green, P.W.C., Stevenson, P.C., Simmonds, M.S.J. and Sharma, H.C. (2003) Phenolic compounds on the pod-surface of pigeonpea, *Cajanus cajan*, mediate feeding behavior of *Helicoverpa armigera* larvae. *J. Chem. Ecol.* **29**, 811–821.
- Griffiths, D.W., Deighton, N., Birch, A.N.E., Patrian, B., Baur, R. and Städler, E. (2001) Identification of glucosinolates on the leaf surface of plants from the Cruciferae and other closely related species. *Phytochemistry*, **57**, 693–700.
- Halkier, B.A. and Gershenzon, J. (2006) Biology and biochemistry of glucosinolates. *Annu. Rev. Plant Biol.* **57**, 303–333.
- Hankin, J.A., Barkley, R.M. and Murphy, R.C. (2007) Sublimation as a method of matrix application for mass spectrometric imaging. *J. Am. Soc. Mass Spectrom.* **18**, 1646–1652.
- Hiruna, K., Onozawa-Komori, M., Takahashi, F., Asakura, M., Bednarek, P., Okuno, T., Schulze-Lefert, P. and Takano, Y. (2010) Entry mode-dependent function of an indole glucosinolate pathway in *Arabidopsis* for non-host resistance against anthracnose pathogens. *Plant Cell*, **22**, 2429–2443.
- Hölscher, D., Shroff, R., Knop, K., Gottschaldt, M., Crecelius, A., Schneider, B., Heckel, D.G., Schubert, U.S. and Svatos, A. (2009) Matrix-free UV-laser desorption/ionization (LDI) mass spectrometric imaging at the sin-

- gle-cell level: distribution of secondary metabolites of *Arabidopsis thaliana* and *Hypericum* species. *Plant J.* **60**, 907–918.
- Hopkins, R.J., Birch, A.N.E., Griffiths, D.W., Baur, R., Städler, E. and McKinlay, R.G. (1997) Leaf surface compounds and oviposition preference of turnip root fly *Delia floralis*: the role of glucosinolate and non-glucosinolate compounds. *J. Chem. Ecol.* **23**, 629–643.
- Huang, X.P. and Renwick, J.A.A. (1994) Relative activities of glucosinolates as oviposition stimulants for *Pieris rapae* and *P. napi oleracea*. *J. Chem. Ecol.* **20**, 1025–1037.
- Huang, X.P., Renwick, J.A.A. and Sachdev-Gupta, K. (1994) Oviposition stimulants in *Barbarea vulgaris* for *Pieris rapae* and *P. napi oleracea*: isolation, identification and differential activity. *J. Chem. Ecol.* **20**, 423–438.
- Hughes, P.R., Renwick, J.A. and Lopez, K.D. (1997) New oviposition stimulants for the diamondback moth in cabbage. *Entomol. Exp. Appl.* **85**, 281–283.
- Jetter, R. and Schäffer, S. (2001) Chemical composition of the *Prunus laurocerasus* leaf surface. Dynamic changes of the epicuticular wax film during leaf development. *Plant Physiol.* **126**, 1–13.
- Kaspar, S., Peukert, M., Svatoš, A., Matros, A. and Mock, H.-P. (2011) MALDI-Imaging mass spectrometry—an emerging technique in plant biology. *Proteomics*, **11**, 1840–1850.
- Kertesz, V. and Van Berkel, G.J. (2009) Fully automated liquid extraction-based surface sampling and ionization using a chip-based robotic nanoelectrospray platform. *J. Mass Spectrom.* **45**, 252–260.
- Kolb, C.A. and Pfündel, E.E. (2005) Origins of non-linear and dissimilar relationships between epidermal UV absorbance and UV absorbance of extracted phenolics in leaves of grapevine and barley. *Plant Cell Environ.* **25**, 580–590.
- Lee, Y.J., Perdian, D.C., Song, Z.H., Yeung, E.S. and Nikolau, B.J. (2012) Use of mass spectrometry for imaging metabolites in plants. *Plant J.* **70**, 81–95.
- van Loon, J.J.A., Blaakmeer, A., Griepink, F.C., van Beek, T.A., Schoonhoven, L.M. and de Groot, A. (1992) Leaf surface compound from *Brassica oleracea* (Cruciferae) induces oviposition by *Pieris brassicae* (Lepidoptera: Pieridae). *Chemoecology*, **3**, 39–44.
- Marazzi, C., Patrian, B. and Städler, E. (2004) Secondary metabolites of the leaf surface affected by sulfur fertilization and perceived by the cabbage root fly. *Chemoecology*, **14**, 87–94.
- Mewis, I.Z., Ulrich, C. and Schnitzler, W.H. (2002) The role of glucosinolates and their hydrolysis products in oviposition and host-plant finding by cabbage webworm, *Hellula undalis*. *Entomol. Exp. Appl.* **105**, 129–139.
- Miles, C.I., del Campo, M. and Renwick, J.A.A. (2005) Behavioral and chemosensory responses to a host recognition cue by larvae of *Pieris rapae*. *J. Comp. Physiol. A.* **191**, 147–155.
- Müller, C. and Riederer, M. (2005) Plant-surface properties in chemical ecology. *J. Chem. Ecol.* **31**, 2621–2651.
- Müller, R., de Vos, M., Sun, J.Y., Sonderby, I.E., Halkier, B.A., Wittstock, U. and Jander, G. (2010) Differential effects of indole and aliphatic glucosinolates on lepidopteran herbivores. *J. Chem. Ecol.* **36**, 905–913.
- Nemes, P. and Vertes, A. (2007) Laser ablation electrospray ionization for atmospheric pressure, in vivo, and imaging mass spectrometry. *Anal. Chem.* **79**, 8098–8106.
- Nemes, P. and Vertes, A. (2010) Atmospheric-pressure molecular imaging of biological tissues and biofilms by LAESI mass spectrometry. *J. Vis. Exp.* **43**, e2097. doi:10.3971/2097.
- Nemes, P., Barton, A.A. and Vertes, A. (2009) Three-Dimensional imaging of metabolites in tissues under ambient conditions by laser ablation electrospray ionization mass spectrometry. *Anal. Chem.* **81**, 6668–6675.
- Nemes, P., Woods, A.S. and Vertes, A. (2010) Simultaneous imaging of small metabolites and lipids in rat brain tissues at atmospheric pressure by laser ablation electrospray ionization mass spectrometry. *Anal. Chem.* **3**, 982–988.
- R Development Core Team (2012) *R: A Language and Environment for Statistical Computing*. Vienna, Austria: R Foundation for Statistical Computing. ISBN 3-900051-07-0, URL <http://www.R-project.org/>.
- Ratzka, A., Vogel, H., Kliebenstein, D.J., Mitchell-Olds, T. and Kroymann, J. (2002) Disarming the mustard oil bomb. *Proc. Natl Acad. Sci. USA*, **99**, 11223–11228.
- Reed, D.W., Pivnick, K.A. and Underhill, E.W. (1989) Identification of chemical oviposition stimulants for the diamondback moth, *Plutella xylostella*, present in three species of Brassicaceae. *Entomol. Exp. Appl.* **53**, 277–286.
- Reifenrath, K., Riederer, M. and Müller, C. (2005) Leaf surface wax layers of Brassicaceae lack feeding stimulants for *Phaedon cochleariae*. *Entomol. Exp. Appl.* **115**, 41–50.
- Renwick, J.A.A., Radke, C.D., Sachdev-Gupta, K. and Städler, E. (1992) Leaf surface chemicals stimulating oviposition by *Pieris rapae* (Lepidoptera: Pieridae) on cabbage. *Chemoecology*, **3**, 33–38.
- Renwick, J.A.A., Haribel, M., Gouinguene, S. and Städler, E. (2006) Isothiocyanates stimulating oviposition by the diamondback moth, *Plutella xylostella*. *J. Chem. Ecol.* **32**, 755–766.
- Ringelmann, A., Riedel, M., Riederer, M. and Hildebrandt, U. (2009) Two sides of a leaf blade: *Blumeria graminis* needs chemical cues in cuticular waxes of *Lolium perenne* for germination and differentiation. *Planta*, **230**, 95–105.
- Sarsby, J., Towers, M.W., Stain, C., Cramer, R. and Koroleva, O.A. (2012) Mass spectrometry imaging of glucosinolates in Arabidopsis flowers and siliques. *Phytochemistry*, **77**, 110–118.
- Scheubert, K., Hufsky, F., Zichner, T., Kai, M., Svatoš, A. and Böcker, S. (2012) Identifying the unknowns by aligning fragmentation trees. *Anal. Chem.* **84**, 3417–3426.
- Schmitt, M., Knopp, G., Materny, A. and Kiefer, W. (1997) Femtosecond timeresolved coherent anti-Stokes Raman scattering for the simultaneous study of ultrafast ground and excited state dynamics: iodine vapour. *Chem. Phys. Lett.* **270**, 9–15.
- Schoonhoven, L.M., van Loon, J.J.A. and Dicke, M. (2005) *Insect-Plant Biology*, 2nd edn. Oxford: Oxford University Press, p. 421.
- Shelton, A.M., Cooley, R.J., Kroening, M.K., Wilsley, W.T. and Eigenbrode, S.D. (1991) Comparative analysis of two rearing procedures for diamondback moth, *Plutella xylostella* (Lepidoptera:Plutellidae). *J. Entomol. Sci.*, **26**, 17–26.
- Shroff, R., Vergara, F., Muck, A., Svatoš, A. and Gershenson, J. (2008) Non-uniform distribution of glucosinolates in *Arabidopsis thaliana* leaves has important consequences for plant defense. *Proc. Natl Acad. Sci. USA*, **105**, 6196–6201.
- Spencer, J.L., Pillai, S. and Bernays, E.A. (1999) Synergism in the oviposition behavior of *Plutella xylostella*: sinigrin and wax compounds. *J. Insect Behav.* **12**, 483–499.
- Städler, E. (1991) Behavioral responses of insects to plant secondary compounds. In *Herbivores: Their Interaction with Secondary Metabolites*, 2nd edn, Vol. 2 (Rosenthal, G.A. and Berenbaum, M.R., eds). New York: Academic Press, pp. 45–88.
- Städler, E. and Reifenrath, K. (2009) Glucosinolates on the leaf surface perceived by insect herbivores: review of ambiguous results and new investigations. *Phytochem. Rev.* **8**, 207–225.
- Städler, E. and Roessingh, P. (1991) Perception of surface chemicals by feeding and ovipositing insects. In *Proceedings of the 7th International Symposium on Insect-Plant Relationships. Symp Biol Hung 39* (Szentesi, A. and Jermy, T., eds). Budapest: Akadémia Kiadó, pp. 71–86.
- Stracke, R., Ishihara, H., Huep, G., Barsch, A., Mehrtens, F., Niehaus, K. and Weissbar, B. (2007) Differential regulation of closely related R2R3-MYB transcription factors controls flavonol accumulation in different parts of the *Arabidopsis thaliana* seedling. *Plant J.* **50**, 660–677.
- Sun, J.Y., Sonderby, I.E., Halkier, B.A., Jander, G. and de Vos, M. (2009) Non-volatile intact indole glucosinolates are host recognition cues for ovipositing *Plutella xylostella*. *J. Chem. Ecol.* **35**, 1427–1436.
- Svatoš, A. (2010) Mass spectrometric imaging of small molecules. *Trends Biotechnol.* **28**, 425–434.
- Svatoš, A. and Mock, H.-P. (2013) MALDI mass spectrometric imaging of plants. In *The Handbook of Plant Metabolomics*. (Weckwerth, W. and Kahl, G., eds). Weinheim, Germany: Wiley-VCH Verlag GmbH & Co. KGaA, pp. 93–110.
- Takai, N., Tanaka, Y., Inazawa, K. and Saji, H. (2012) Quantitative analysis of pharmaceutical drug distribution in multiple organs by imaging mass spectrometry. *Rapid Commun. Mass Spectrom.* **26**, 1549–1556.
- Traynier, R.M.M. and Truscott, R.J.W. (1991) Potent natural egg-laying stimulant for cabbage butterfly *Pieris rapae*. *J. Chem. Ecol.* **17**, 1371–1380.
- Vrkslav, V., Muck, A., Cvacka, J. and Svatoš, A. (2010) MALDI imaging of neutral cuticular lipids in insects and plants. *J. Am. Soc. Mass Spectrom.* **21**, 220–231.
- Walter, A., Erdmann, S., Bocklitz, T., Jung, E.M., Vogler, N., Akimov, D., Dietzek, B., Roesch, P., Kothe, E. and Popp, J. (2010) Analysis of the cytochrome distribution via linear and nonlinear Raman spectroscopy. *Analyst*, **138**, 908–917.

SUPPORTING INFORMATION LEGENDS

Figure S1 Negative mode MALDI-TOF/MS spectra of *A. thaliana* leaf surfaces as in Figure 1, (A) adaxial and (B) abaxial, but depicting an extended 400- 600 m/z mass range showing putative cutin fragments. MS traces for each surface are normalized to the largest peak.

Figure S2. Quantification of glucosinolates on *A. thaliana* leaf surfaces by MALDI-TOF/MS measurements. Depicted are calibration curves of internal standard (sinigrin, 2-propenylglucosinolate) spotted in different concentrations on the surface. Both (A) linear ($r^2 = 0.95$) and (B) logarithmic ($r^2 = 0.92$) fits with the data are given. Points represent means (\pm standard error) of five measurements at each concentration and are shown with 99% confidence intervals (CI).

Figure S3. Evidence for the presence of a flavonol diglycoside on *A. thaliana* leaf surfaces as shown by m/z 577 in the LAESI trace. Depicted is the fixed precursor ion scan for m/z 577. Isolated ion was fragmented in the linear trap of an Orbitrap XL instrument using normalized energy of 15 eV. Molecular compositions calculated for the precursor and fragments are consistent with the structure of kaempferol-3,7-O- α -L-dirhamnopyranoside.

Figure S4. Comparison of glucosinolate content of *A. thaliana* leaf surface vs. leaf interior via LESA analysis of the abaxial surface (top panel), obtained by positioning tip depositing droplet of extraction solution (water:propan-2-ol: NH_4OH - 79.9:20.0:0.1), and the leaf interior (bottom panel), obtained by positioning tip to damage leaf surface before depositing droplet of the same extraction solvent. Ion intensities are normalized to the intensity of the internal standard (sinigrin, m/z 358).

Figure S5. Distribution of *P. xylostella* eggs in an oviposition choice assay using glucosinolate mixtures. Mixtures were prepared from purified 4MTB, 4MSOB and I3M at

concentrations found on either the abaxial or adaxial leaf surface (A) or with concentrations of 4MTB and I3M 2- and 4-fold greater, respectively (B). A newly eclosed male and female *P. xylostella* were released in a breeding arena which had a Parafilm strip with either an abaxial or adaxial concentration of the glucosinolate mixture and a strip with a solvent control, or, the arena had strips with both abaxial and adaxial concentrations. After 48 h, eggs were counted and results expressed as percentage of eggs found in each location and were statistically analyzed after arcsine square root transformation with an ANOVA. The females significantly choose the glucosinolate-covered strip over the control, but only when the elevated concentrations of 4MTB and I3M were applied.

Method S1. Laser-assisted electrospray ionization (LAESI) mass spectrometry.

Method S2. Liquid extraction surface analysis (LESA).

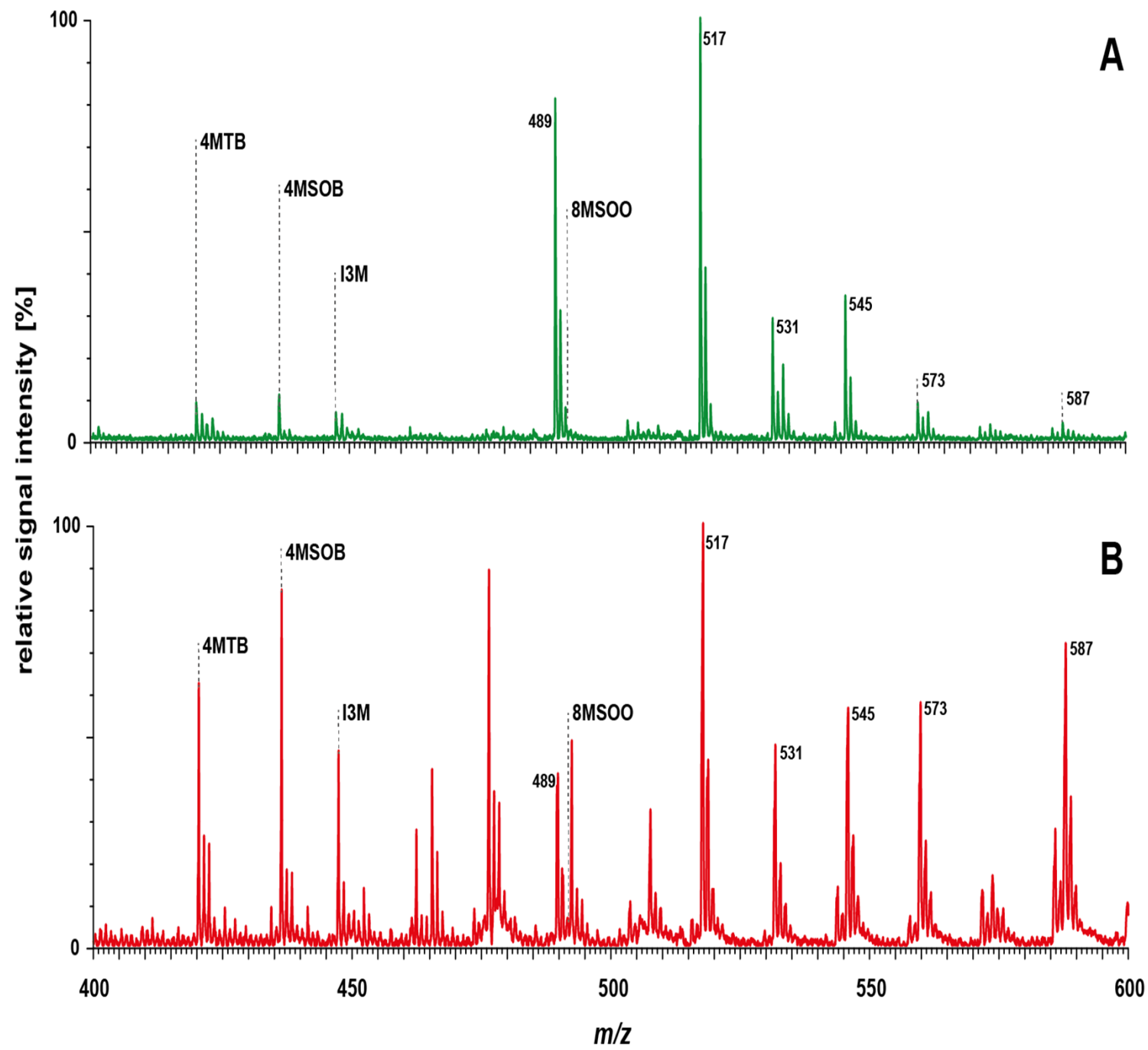


Figure S1

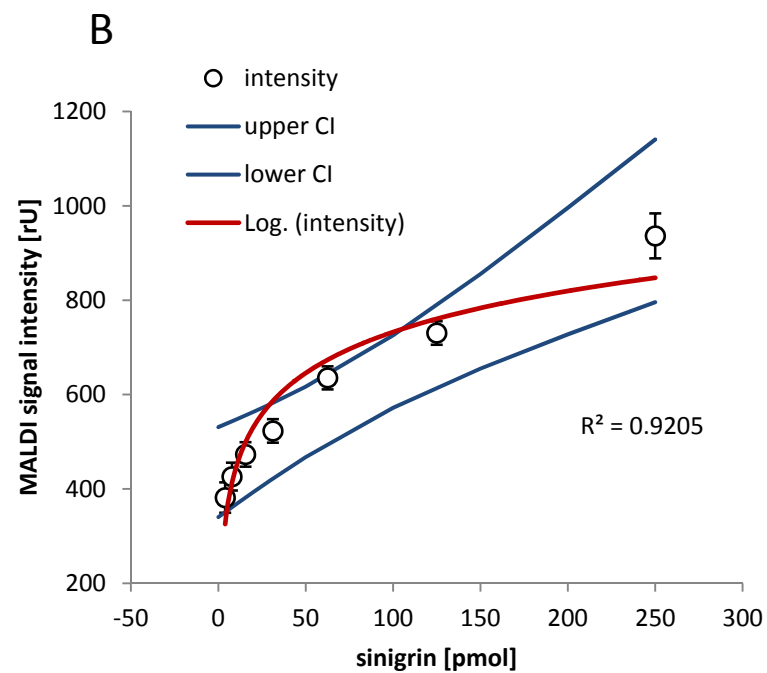
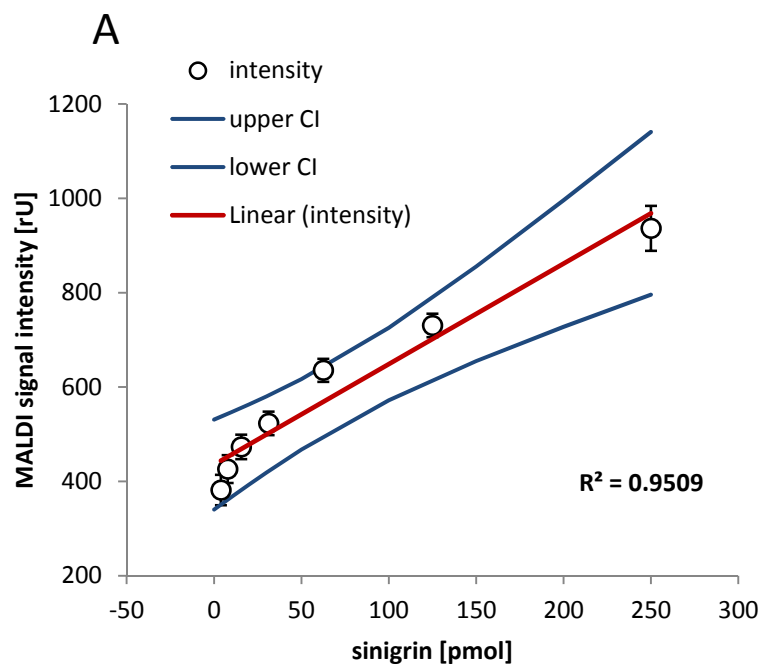


Figure S2

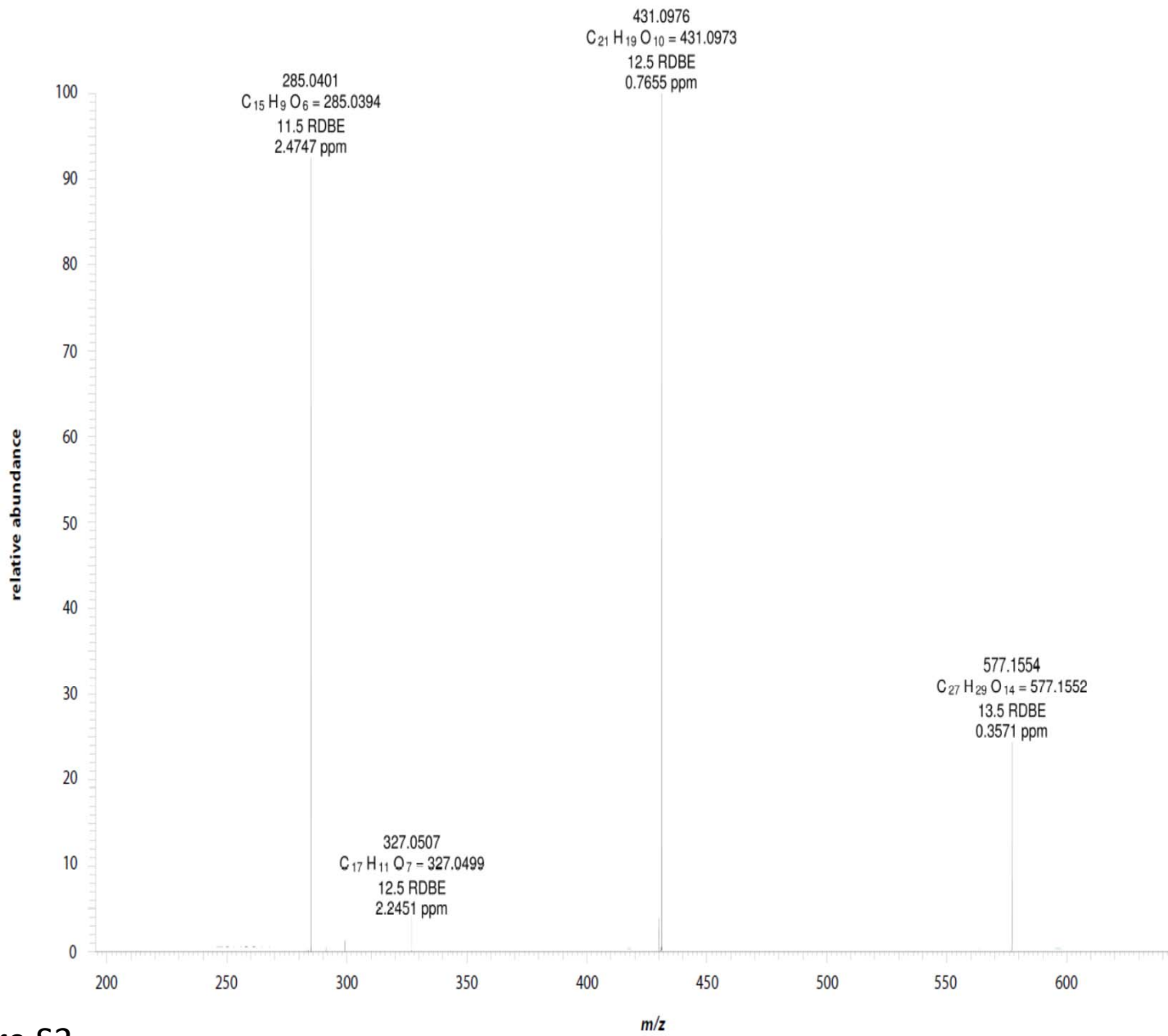


Figure S3

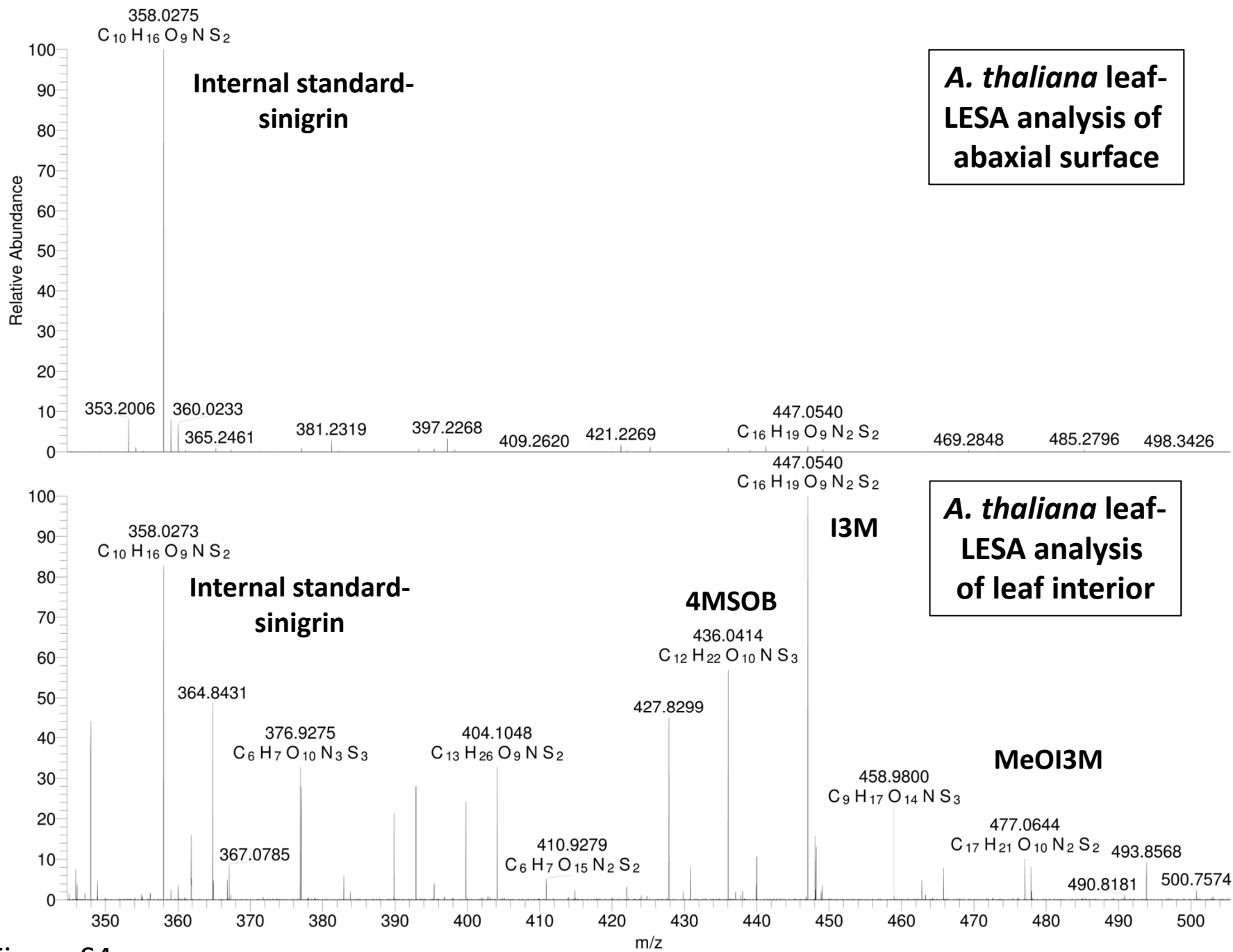


Figure S4

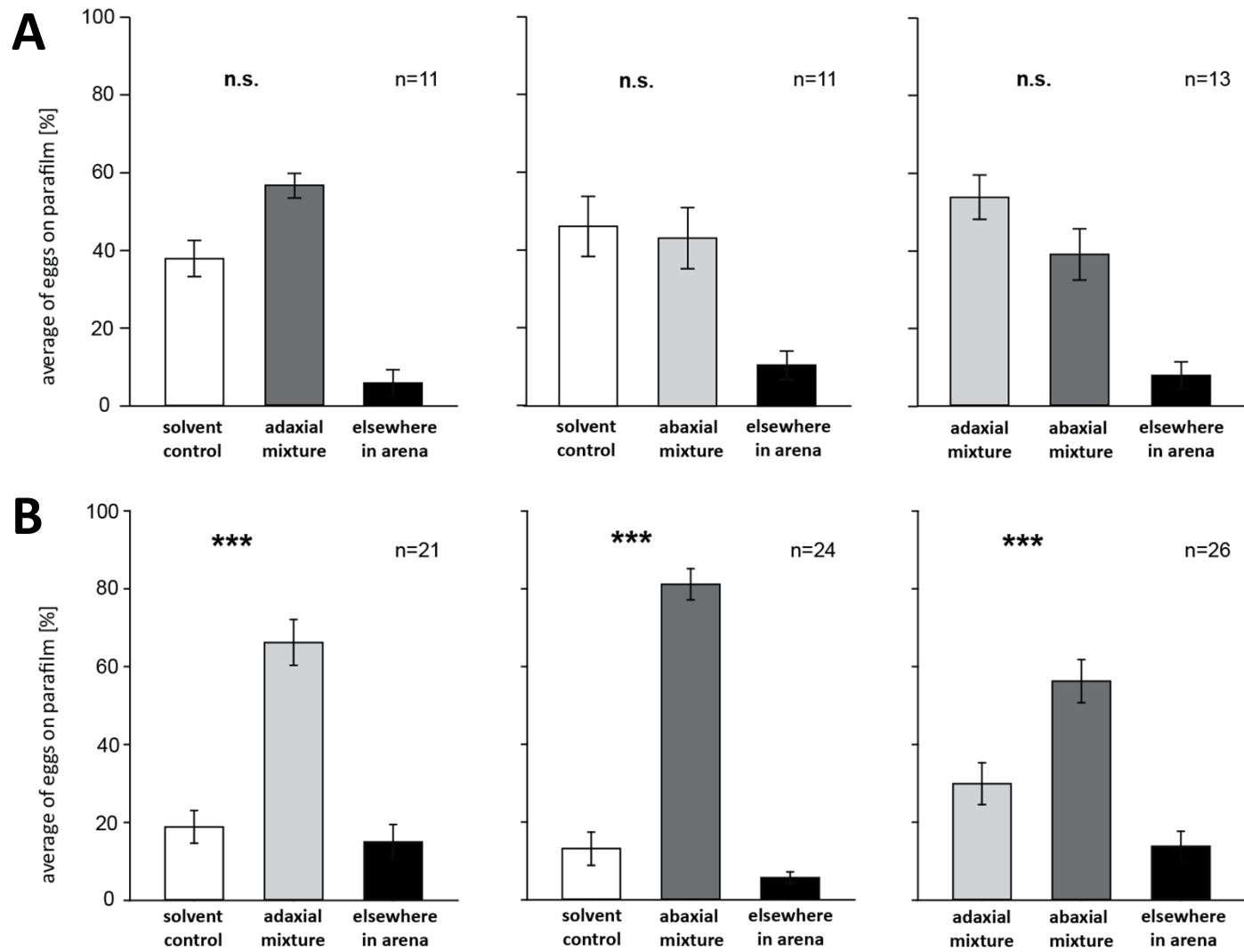


Figure S5

Method S1. Laser-assisted electrospray ionization (LAESI) mass spectrometry.

A. thaliana leaves detached from two to three week-old plants were mounted on a microscope slide with their abaxial surface using a double-sided tape (Scotch). No chemical treatment was performed during sample preparation and special care was paid to avoid physical damage to leaf areas of interest. Leaves were analyzed *in situ* using a previously described protocol for LAESI-MS (Nemes and Vertes, 2007, 2010; Nemes et al, 2010). A tapered tip metal emitter (50 or 100 μm i.d. and 320 μm o.d., New Objective, Woburn, MA, USA) was positioned 10 mm from the inlet of a mass spectrometer. Solutions of 50% methanol containing 0.1% (v/v) ammonium hydroxide were supplied through the emitter at a rate of 300-450 nL min^{-1} and electrosprayed at 3000-3300 V potential. A Nd:YAG laser-driven optical parametric oscillator (Vibrant IR, Opotek Inc., Carlsbad, CA, USA) generated laser pulses at a wavelength of 2.94 μm (mid-infrared region) at a rate of 10 Hz. The beam was focused at the sample at 90° incidence \sim 2-4 mm downstream from the emitter tip using a ZnSe or CaF₂ plano-convex lens (Infrared Optical Products, Farmingdale, NY, USA). Microscopic observations revealed that irradiation with a large pulse of 4.9 ± 0.2 mJ energy lead to tissue ablation in circular spots 250-300 μm diameter.

Air-born particulates generated by irradiation were intercepted by the electrospray 12-15 mm above the sample surface. The ions generated were analyzed by an orthogonal time-of-flight mass spectrometer (AccuTOF JMST100LC, JEOL Ltd., Peabody, MA, USA) or for higher resolution and tandem MS capabilities by a Q-TOF system (QTOF Premier, Waters Co., Milford, MA). Mass spectrometric data were acquired between m/z 100 and 1000 at a rate of 1 spectrum sec^{-1} . Both MS instruments were externally m/z -calibrated with polyethylene glycol polymer ions or collision-activated dissociation (CAD) fragments of the doubly protonated human [Glu₁]-fibrinopeptide B peptide (Sigma-Aldrich), ensuring a mass accuracy of \sim 5 mDa and a mass resolution of $\Delta m/m > 6000$. Tandem MS experiments to aid in chemical assignments were

performed with argon collision gas at 4 μ bar pressure with a collision energy of 15-30 eV.

Glucosinolate ions detected from the leaves were assigned based on accurate masses, isotope distribution patterns, and molecular fragmentation behavior under CAD conditions. Chemical identifications were further confirmed with chemical standards.

Method S2. Liquid extraction surface analysis (LESA).

A. thaliana leaves from 4 week old plants were attached to a microscope slide with double-sided tape and secured in the sample holder of a nanoelectrospray source for mass spectrometry (Triversa Nanomate, Advion, Ithaca, NY, USA). The surface compounds were extracted from the leaf surface by depositing 1 μL of a water/propan-2-ol/ammonium hydroxide (79.9/20/0.1) solution from a conductive plastic tip positioned ca 100 μm above the surface (z-coordinate 8.8 mm) and the deposited droplet was left on the leaf surface for 10 sec. The extract was aspirated back into the plastic tip and sprayed into mass spectrometer via an automated, chip-based electrospray unit (Nanomate, Advion) using 1.7 kV negative potential. For the quantitative measurements, 2-propenylglucosinolate was used as internal standard dissolved in the extraction solution (1 ng/ μL). The sample was obtained in two ways. In the first one the surface was extracted as above (z-coordinate 8.8 mm). In the second way, a pipette tip first damaged the leaf surface by adjusting the z-coordinate setting to 8 mm. Then the tip was raised up to 8.8 mm and the damaged section was extracted using an identical protocol as above.

The resulting ions were analyzed by two different hybrid mass spectrometers. The first set of experiments was performed on Synapt HDMS system (Waters) operated in a full scan negative ion mode using 100-800 m/z mass range and V-TOF reflectron at $\Delta m/m = 12,000$ resolution acquiring 1 mass spectra sec^{-1} for ca 1 min for each sample spot. The spectra were collected using MassLynx 4.2 software and presented as an average of 30 scans. The chemical identity of each ion was confirmed by recording CID spectra selecting appropriate precursor ions using a 1 Da isolation window and fragmenting them in the T-wave region of the trap using 10-35 V collision energy depending on compound type.

Similar experiments and quantification measurements were performed on Orbital XL mass spectrometer (ThermoFisher, San Jose, CA, USA) operated in negative ion mode. Ions

accumulated in the linear trap (3 microscans, 100 msec filling time) and were analyzed in the Orbitrap analyzer at 2 microscans, 500 msec filling time, and $\Delta m/m = 15,000$ resolutions.

Excalibur software was used for data collection and analysis. For quantitative measurements, areas showing good signals both for the sample glucosinolate and the 2-propenylglucosinolate internal standard were averaged and the ion intensities compared.